Chapter 2: Variability in Horizontal Current Velocities in the Central and Eastern Equatorial Atlantic in 2002

Abstract

Near-surface current velocity data from the PIRATA buoy at 23ºW in the year 2002 were re-examined and compared to simultaneous unpublished velocity data at 10ºW, near the surface. Strong 7-day period fluctuations were observed in the zonal velocity component and in temperature records at 23ºW. The large temperature fluctuations near the thermocline depth suggest a vertical velocity component at the same 7-day period. The 7-day period signals occurred in June/July simultaneously with the seasonal upwelling.

The meridional velocity component presented similar spectral contents at 23ºW and at 10ºW. Two distinguishable quasi-periodic signals were observed in the meridional component at both locations: the first signal occurred in the spring, had a periodicity of about 14 days, was subsurface intensified, and had the characteristics of a mixed Rossby–gravity wave. The second signal occurred three times in the year, once in winter 2001-2002, another in summer, and another during fall 2002, had a periodicity of about 20 days, was strongest close to the surface, and was the result of the passage of tropical instability waves (TIWs). This can be confirmed through satellite SST data which show the same periodicities as the meridional velocity records, and spatial structure in accordance with the TIW–SST signature. The summer of 2002, showed different TIW-SST patterns depending upon location, suggesting the existence of different types of TIWs. Finally, the analysis of SST and surface wind data, suggests that variability in the

current meter data for the year 2002 was mainly due to current instabilities, except around boreal spring, where intraseasonal variability in surface winds was strongest.

2.1. Introduction

At intraseasonal time scales, velocity currents near the surface in the equatorial oceans are dominated by quasi-periodic fluctuations associated with the passage of equatorially trapped waves. During the FOCAL/SEQUAL experiment (1982-1984), ocean velocity time series were obtained at different locations in the equatorial Atlantic and allowed the documentation of propagating equatorially trapped waves, in particular of Tropical Instability Waves (TIWs) (Weisberg, 1984; Weisberg and Weingartner, 1988). Since then, velocity observations at the equator in the Atlantic have been rather scarce and confined to single locations (e.g. 23ºW in Grodsky et al. 2005; 23ºW in Brandt et al. 2006; 10ºW in Bunge et al. 2006).

In December 2001, within the Pilot Research Moored Array in the Tropical Atlantic (PIRATA) project (http://www.brest.ird.fr/pirata/piratafr.html), a mooring with an ADCP (Acoustic Doppler Current Profiler) was deployed near the surface at 23ºW. Simultaneously, a Vector Averaging Current Meter (VACM) was deployed at 10ºW by the French program PATOM (Programme ATmosphère et Océan Multi-échelles) at 154 m. The combined data set allows for comparisons of near-surface (upper 150 m) equatorial signals at two different locations, 10ºW and 23ºW during the year 2002.

Most intraseasonal current velocity oscillations in the equatorial oceans are either wind forced or are the result of instabilities produced by the shear of zonal currents (Kessler, 2004). In the eastern part of the basin, wind-forced oscillations having a 14-day period have been observed in near surface oceanic records by Garzoli (1987), Houghton and Colin (1987) and Bunge et al.

(2006). In the last two papers, the structure of the oscillation was surmised to be a Rossby-gravity wave. In the atmosphere, the 14-day period oscillation has been observed in both horizontal wind velocity components. The 14-day period wind oscillations occurred during spring at the equator, when the Intertropical Convergence Zone (ITCZ) is at its most southern position. This is consistent with Grodsky et al. (2003) who found a biweekly oscillation in the zonal wind component associated with a near surface westerly jet close to the African continent, which latitudinal position varied with the meridional migration of the ITCZ.

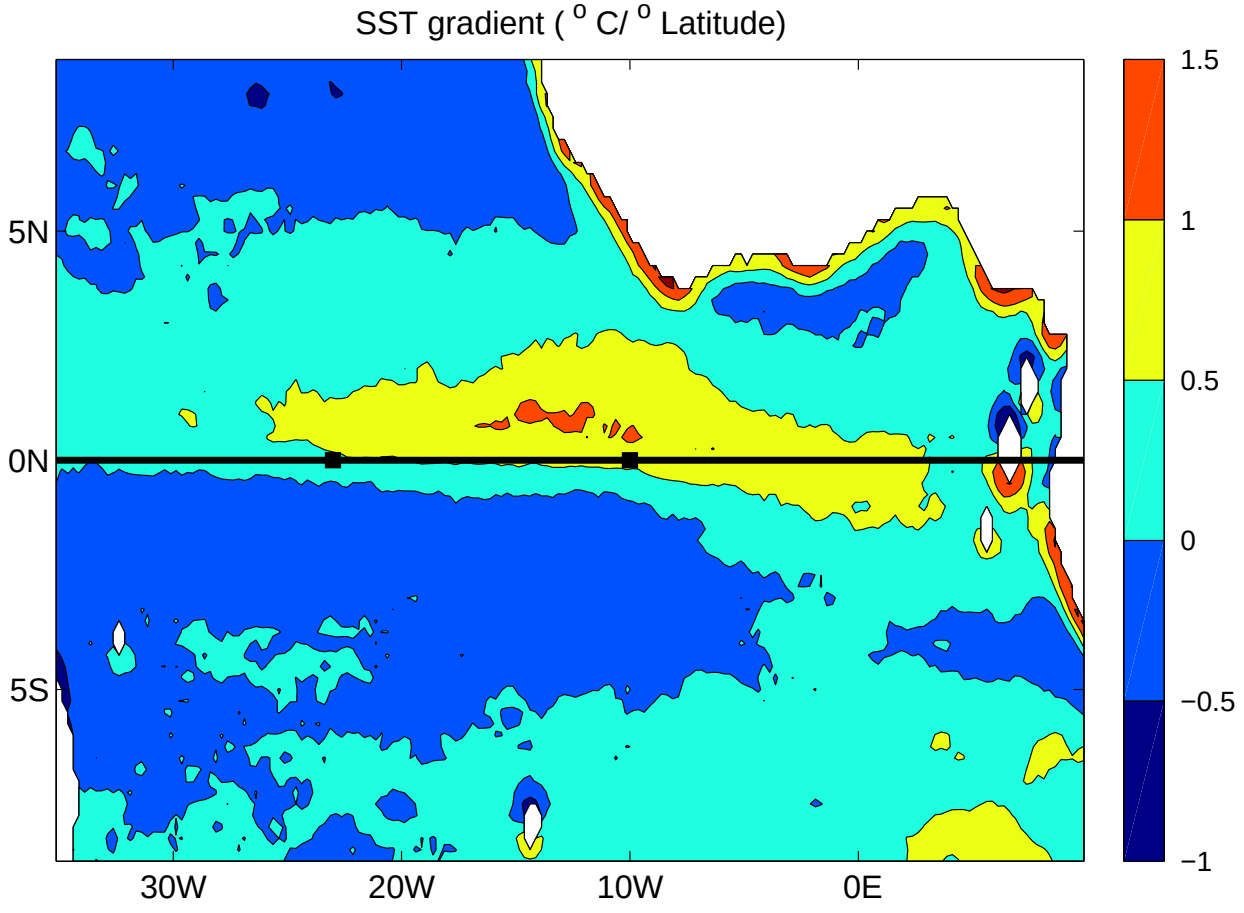

Figure 1: PIRATA/PATOM mooring sites (■) at 23°W and 10°W over a map of mean SST gradient distribution in 2002. The SST meridional gradient was estimated using satellite data described in section 2.

The oscillations resulting from zonal current shears are the TIWS. In the Atlantic Ocean, these oscillations occur mainly in summer, along with the intensification of the South Equatorial Current (SEC), but they can also be seen in late fall (e.g., Caltabiano et al. 2005). They have central periodicities of 25 days, zonal scales of around 1100 km, phase speed of around 0.5 m/s and are strongest in the center of the Atlantic basin (Weisberg and Weingartner, 1988). Their eastward limit is however not well established. Some observations suggest their presence as east as 4ºW (Weisberg et al., 1979), but east of 10ºW, the waves have been observed to have shorter zonal scales (~600 km) and smaller meridional displacements, and to be more transient (Legeckis and Reverdin, 1987). These differences in TIWs spatial-structure suggest the possibility of distinct TIWs depending on the region. In the Pacific Ocean, where TIWs have been most studied, different regions of TIW energy transfer have been detected (Luther and Johnson, 1990). Furthermore, Lyman et al. (2006) found two distinct TIWs presenting different periods, cross-equatorial structure, and dynamics. The first wave is better represented on meridional velocity measurements near the equator, has a central periodicity of 17 days, and a mixed Rossby gravity wave/surface trapped instability structure. The second wave has a strong signature on subsurface temperature data at 5ºN, presents a central periodicity of 33 days, and has the structure of an unstable first meridional mode Rossby wave.

The purpose of the present study is to further describe the intraseasonal variability (5 to 107-day period) in the Atlantic of near surface (upper 150 m) equatorial signals, by analyzing simultaneously velocity data from two different locations, 10ºW and 23ºW, together with satellite sea surface temperature (SST) and scatterometer surface wind velocity data. Since the FOCAL/SEQUAL years, satellite observations have improved with the development of microwave radiometry -which permits measurements of SST through clouds- and surface wind

velocity measurements. Satellite data bring information about the spatial structures of some velocity oscillations, their eventual propagation, their origin and fate, and therefore were useful to support the analysis of the current-velocity observations. Because the data clearly contain quasi-periodic fluctuations which may be modulated in time or may occur only in certain portions of a time series, we used a wavelet-based technique to isolate and extract the signals of interest.

The present paper is organized as follows: section 2 presents the data and data analysis; section 3 describes the near-surface velocity variability and compares it to signatures in SST; and the concluding section discusses and synthesizes the results.

2.2. Data and Data Analysis

Horizontal current-velocity data were obtained between December 2001 and December 2002 from two moorings in the equatorial Atlantic, one at 0ºN, 23ºW, the other at 0ºN, 10ºW (Fig. 1). At 23ºW, a PIRATA acoustic Doppler current profiler (ADCP, Workhorse Sentinel 300 kHz – 4-m cell size and time step of 1 hour) sampled the upper 120 m of the water column (see Fig. 1 in Grodsky et al., 2005), and at 10ºW, a PATOM VACM sampled the horizontal velocity at around 154 m (Fig. 2). Besides the velocity data, simultaneous temperature and salinity data from the upper 120 m of the water column were obtained from the PIRATA buoy at 23ºW (see Fig. 1 in Grodsky et al., 2005) but these data were not available at 10ºW in 2002.

The Vector Averaging Current Meter (VACM; Fig. 2) was calibrated at the Institut français de recherche pour l'exploitation de la mer (Ifremer) for velocity and pressure; details of the data calibration and validation can be found in Kartavtseff (2003). The hourly data were averaged

over 25 hours to remove tidal frequencies and re-sampled to provide daily resolution. Table 1 shows the location, depth and duration of the time-series.

Location	Depth	Starting Date	Ending Date	Days of good data
23ºW	ADCP (12-120 m)	13.Dec.01	21.Dec.02	372
10ºW	154 m	11.Dec.01	29.Dec.02	383

Table 1: Location, depth and number of days of good data of the current meters from PIRATA and PATOM moorings.

Data were analyzed using the wavelet-based technique described by Bunge et al. (2006). This technique isolates significant "ridges" (regions in the wavelet transform with high amplitudes and relatively long duration), and thus the time-varying period of the main components[1]. Once the main components of the signals were extracted, they were classified in period classes. The period range we observed was from 5 to 107 days. The period classes were chosen taking into account other equatorial Atlantic observations (e.g Garzoli, 1987) but also emphasizing that the main components found in these data would be represented by one of these classes. Those classes are: 5 to 10, 10 to 17, 17 to 38, 38 to 72 and 72 to 107 days. Figures 2 and 3 display the number of oscillations for each period band in each time series. The zonal component showed little quasi-periodic oscillations, except at 23°W where 5 to 7-day period oscillations were seen in the upper 120 m. The meridional velocity component was dominated by 10 to 17 and 17 to 38-day period oscillations at both locations. Temperature time series showed the same variability as the zonal velocity component while the salinity time series were well correlated with the meridional motions (Fig. 3). For all in-situ data, there were no quasi-periodic fluctuations in the periods between 38 and 107 days.

[1] Software tools for this analysis can be found at http://www.jmlilly.net/jmlsoft.html

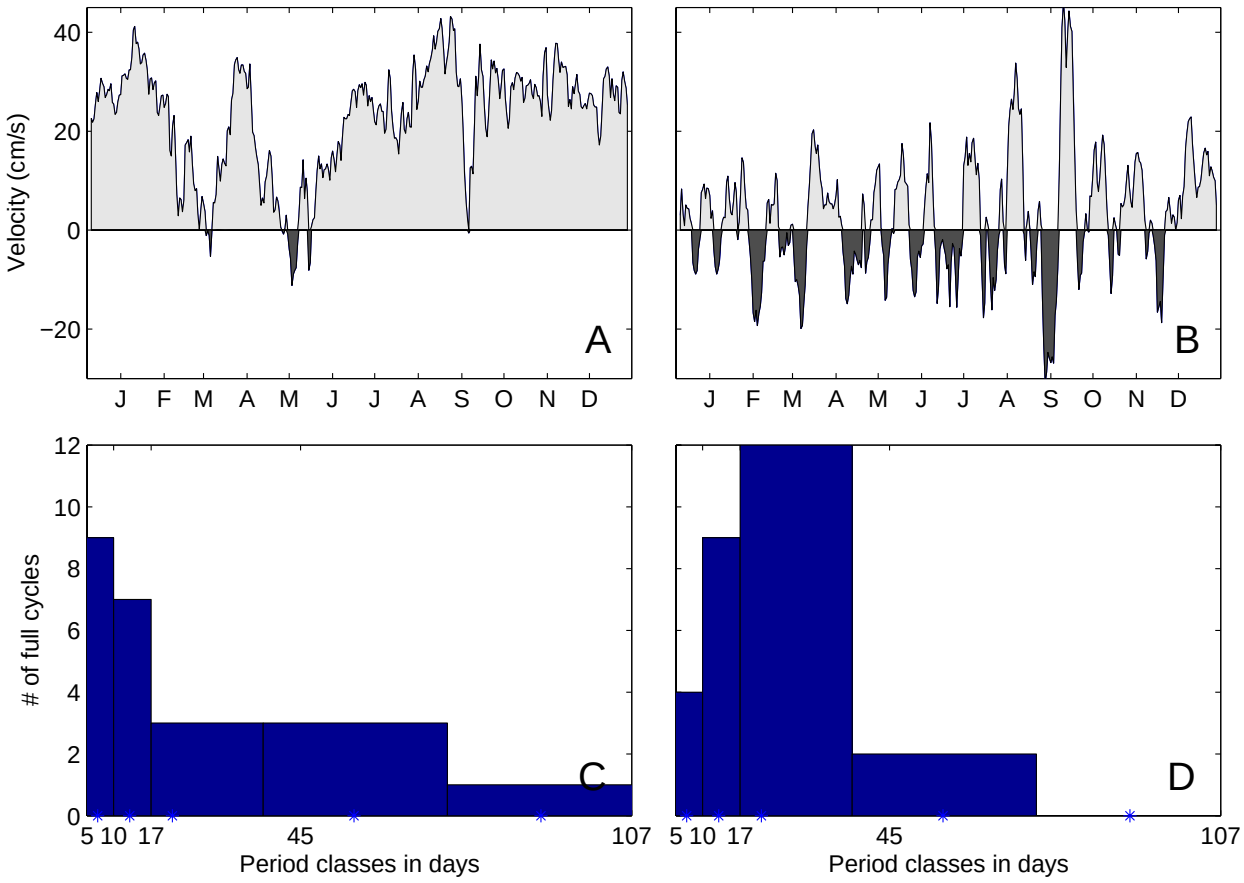

Figure 2: Current-velocity data at 10ºW. *Upper panel*: VACM zonal (left) and meridional (right) velocity components; the depth of the VACM was 154 m. *Lower panel*: Histogram showing the approximate number of full cycles in each period class for the zonal (left) and meridional (right) velocity components of the VACM at 154 m depth.

In order to document the spatial structures associated with the observed velocity fluctuations, Tropical Rainfall Measuring Mission (TRMM) – Microwave Imager (TMI) SST data were examined over the region between 9°S and 9ºN, and 35°W and 10ºE during 2002 (Fig. 1). This SST product is the result of an optimal interpolation with a temporal and a spatial resolution of 1 day and of 0.25º, respectively (http://www.remss.com/sst). Surface wind horizontal velocities were also explored using a daily QuikSCAT product with horizontal resolution of 1/2º which is available at www.ifremer.fr/cersat/en/data/overview/gridded/mwfqscat.htm. SST and wind velocity time series were filtered using a digital Butterworth band pass filter to retain signals

with periods in the band of 5 to 38 days, which is the period band in which all quasi-periodic oscillations in the current-velocity time-series were found.

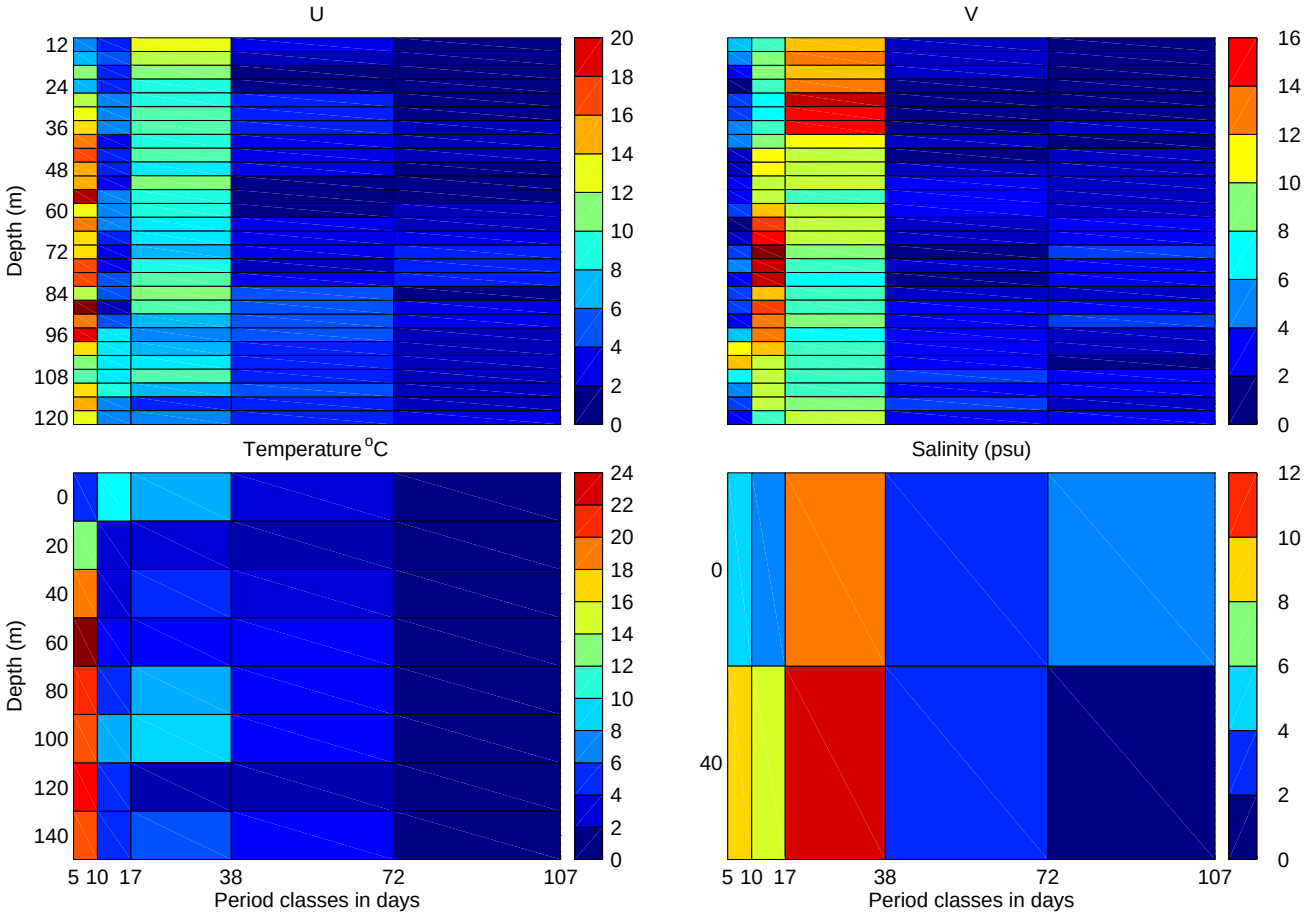

Figure 3: Histograms showing the approximate number of full cycles of each period class, for every measured depth for the different variables measured near the surface at 23º W. *Top-left*: zonal velocity component; *top-right*: meridional velocity component; *bottom-left*: temperature at levels 0, 20, 40, 60, 80, 100, 120 and 140 m. Series at 20, 60 and 120 had gaps. *Bottom-right*: salinity at levels 0 and 40 m.

2.3. Near-Surface (upper 200 m) Variability

2.3.1. In Situ Measurements

The zonal velocity component had few quasi-periodic signals in the intraseasonal time scales when compared to the meridional component. At 23ºW, the zonal velocity component exhibited

20–30-day period oscillations in the mixed layer related to TIWs as described by Grodsky et al. (2005), and fluctuations with a periodicity of approximately 7 days (Fig. 3 ; upper-left panel, period class : 5–10 days). The 7-day signal also had a signature in the temperature record (Fig. 3; lower-left panel). During June and July and at around 60 m depth, close to the thermocline depth, the amplitudes of these 7-day fluctuations reached 25 cm/s in velocity and 2.5ºC in temperature. An increase (decrease) in temperature was associated with a westward (eastward) velocity. Since the strong fluctuations in temperature cannot be surmised to the zonal displacements alone, and since the strongest temperature fluctuations are seen at the thermocline depth, a vertical velocity component at this period must exist. In the record at 10ºW and at 154 m depth, no meaningful 7-day oscillations were observed. During year 2000, intermittent packets of 7-day period oscillations were observed in the zonal velocity component at 10ºW and at 30 m depth (Bunge et al., 2006).

In the meridional component, fluctuations at 23ºW near the surface showed strong similarities with fluctuations observed at 154 m depth at 10ºW. There were two distinguishable signals; the first one had a period of approximately 14 days (period class 10-17 days), it started in mid-February and persisted till the end of April 2002, and was not described in the previous papers using these data (Provost et al., 2004; Grodsky et al., 2005; Giarolla et al., 2005). The second and strongest one had a periodicity of 20–30 days, occurred principally in summer, where it had been associated with the passage of TIWs (Grodsky et al., 2005), but was also observed in December 2001-January 2002 and around November 2002.

The 14-day period signal was coherent in the meridional component throughout the upper 120 m and was also observed in the salinity records for the surface and for the mixed layer (Fig. 3; upper and lower right panels). Maximum meridional velocity amplitudes associated with the

14-day-period fluctuations were found at around 40 m depth, with values of up to 0.45 m/s. There was a time-lag of approximately 5 days between fluctuations at 120 m and at 16 m depths, with the former preceding the latter (Fig. 4; upper panel), implying upward phase propagation. The energy of the signal in the upper 50 m of the water column showed downward radiation (Fig. 4; lower panel). At 10ºW, 14-day-period fluctuations were roughly in phase with those at 23ºW and 120 m. However, one has to be cautious when comparing phases since the two time-series were at different depths and on different isopycnal surfaces. The 14-day signal was consistent with a surface-forced mixed Rossby-gravity wave of vertical mode one or two because a) of its 14-day period, b) lack of variability at that period in the zonal component, c) upward phase propagation and downward energy radiation, and d) an apparent long zonal scale.

TIWs' signatures were observed at both locations during the summer. As for the 14-day period oscillations, the vertical structure of the TIWs presented a phase shift of approximately 5 days between fluctuations at 120 m and at 16 m depths showing upward phase propagation. Zonally, one cannot relate individual TIW-induced fluctuations at 10ºW to fluctuations at 23ºW with in-situ velocity measurements at only these two locations. The reason is that TIWs are generated around 17ºW (Jochum et al. 2004), and akin westward propagating mixed Rossby-gravity waves, the phase velocity propagates westward while the group velocity propagates eastward. TIW-induced fluctuations can thus be observed at 10ºW only if the energy has propagated enough to the east. Such propagation can however easily be documented and tracked with SST data, as shown in the next subsection.

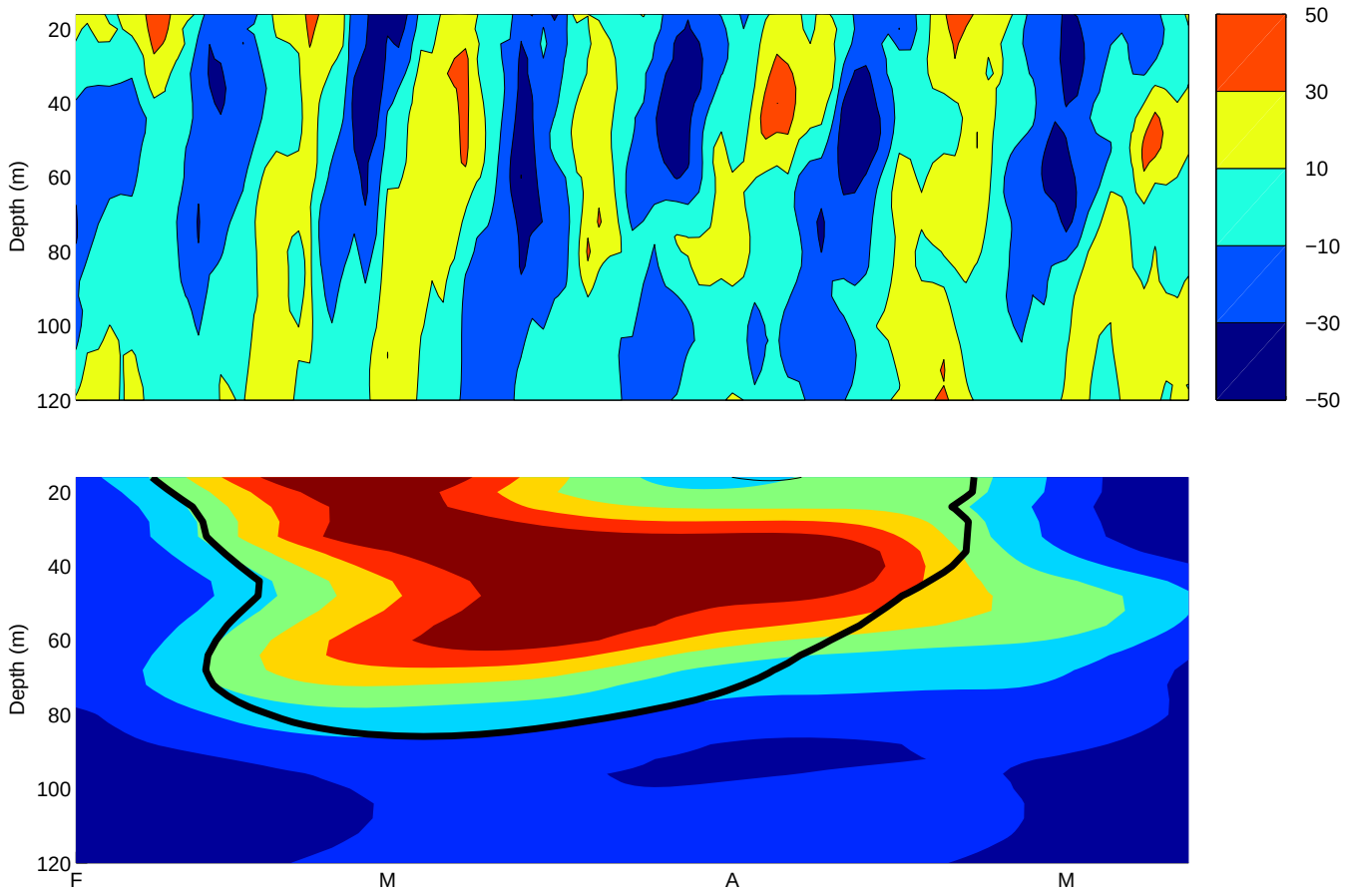

Figure 4: *Upper panel*: meridional current-velocity component (in cm/s) during the 14-day-period fluctuations in the ADCP data at 23W; upward phase propagation is evident. *Lower panel*: normalized wavelet energy of the meridional velocity component for the 12–15-day band; the *black contour* indicates the 95% significance level; downward energy radiation is observed.

2.3.2. Comparison to Satellite SST

TIWs have a strong SST signature and can be easily detected with satellite data. The large spatial and temporal coverage of satellite SST data sets permits to follow the time evolution of SST anomalies and examine their spatial structure. Figure 5 shows two Hovmoller diagrams of filtered SST data at latitude 0.125°N and 1.125°N which describe the time evolution of the SST anomalies. The spatial distribution of the maximum SST gradient is such that, west of 10ºW, it is zonal at ~1ºN and that, east of 10ºW, it is tilted across the equator towards the southeast (Fig. 1).

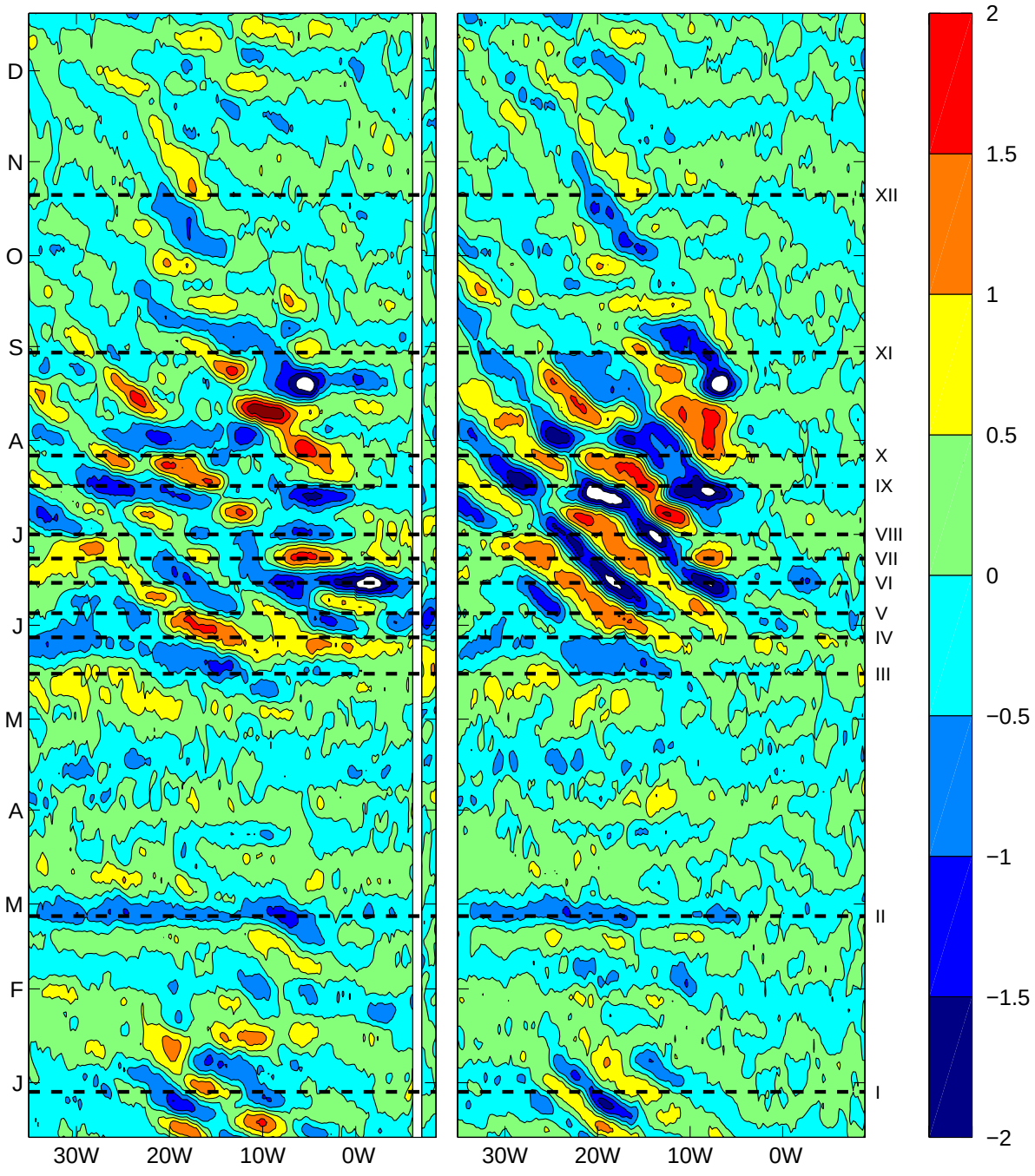

Figure 5: Two SST Hovmoller diagrams at latitudes 0.125º N (left) and 1.125º N (right). SST data has been band pass filter to retain variability in the 5 to 38 day period band. The temperature scale is in º C, the months on the y-axis are set in the first day of each month, and the roman numbers in the right indicate the time for the snapshots on figure 6.

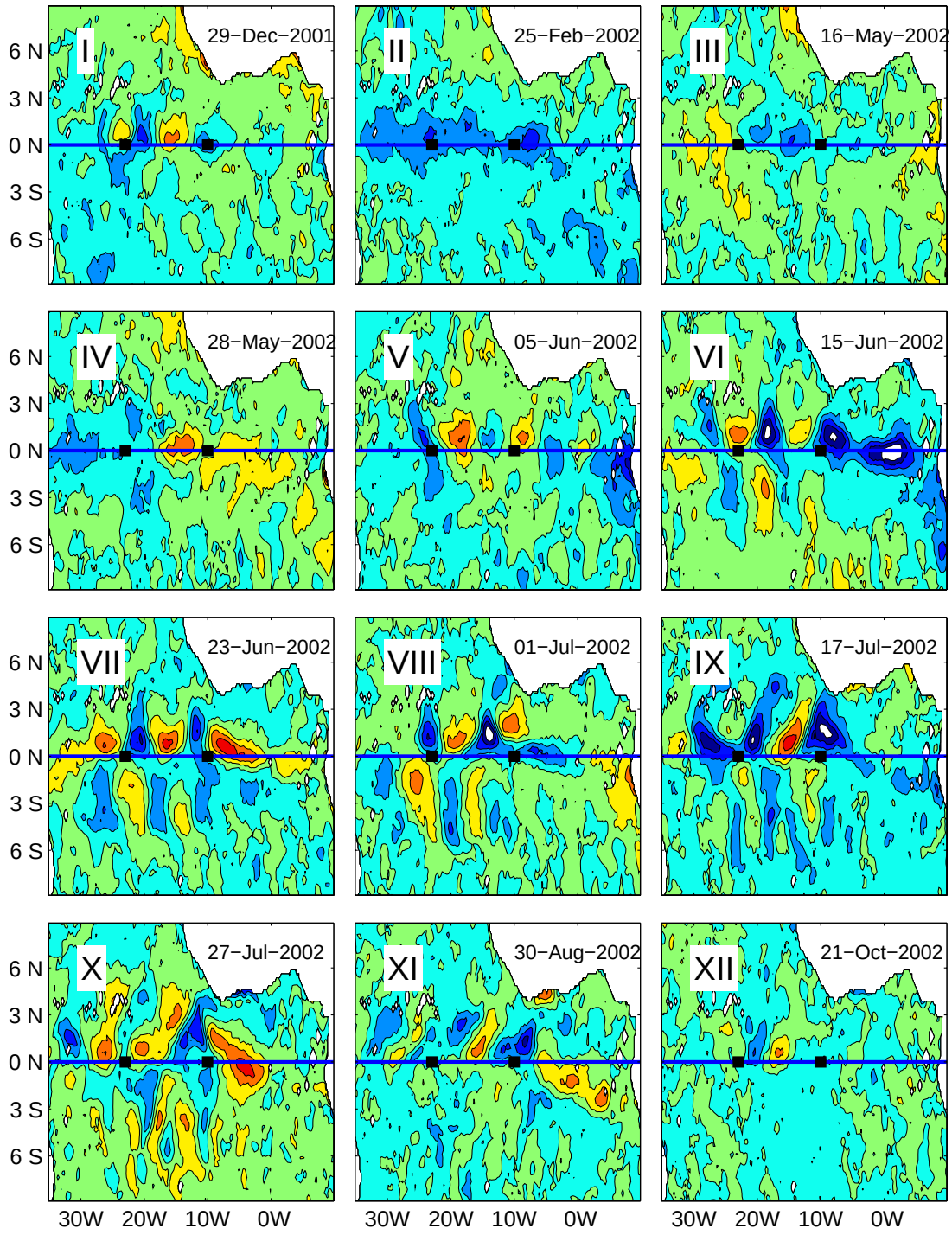

Figure 6: Filtered SST snapshots visualizing the spatial structure of some of the SST anomalies detected in the Howmoller diagrams presented in figure 5. The roman numbers correspond to the marks on the time line in figure 5. For the color code, see the color bar in figure 5.

This implies that variability due to the TIWs in the center of the basin is highly visible in the Hovmoller diagram at 1.125°N while variability taking place in the east of the basin is better illustrated in the Howmoller diagram at 0.125ºN. Both Hovmoller diagrams show TIW-like westward propagating anomalies during December 2001 and January 2002, with a periodicity of 20–30 days and phase propagation of about 0.5 m/s. Between February and beginning of May 2002, basin-scale anomalies showing no propagation and relatively small SST amplitudes were observed. Then, in May, just before the TIW season, eastward propagating anomalies were seen in the west of the basin (Fig. 5). The time period between June and August presented the strongest SST signals. West of 10ºW, there was the unmistakable signature of TIWs. The Hovmoller diagram at 1.125ºN shows the westward phase velocity of TIWs and their eastward energy radiation. TIW events are seen to have originated around 18ºW in early June, and as the energy radiated eastward, their signatures reached 10ºW in mid June. East of 10ºW, however, the

SST anomalies showed no zonal propagation (Fig. 5, left panel). These eastern features could also be the result of instabilities, but, since they present no zonal propagation, they are different from the well known westward propagating TIWs. Both Hovmoller diagrams show westward propagating anomalies from June to mid July in the center of the basin. Afterward, the 1.125ºN diagram shows a discontinuity in the propagation pattern of the SST anomalies and the 0.125ºN diagram shows anomalies which propagated much slower than they initially did. A possible explanation for such changes on the TIW propagating patterns is the coexistence of two different signals at the same time, as it will be discussed in the next section. Later, during October and November, westward propagating TIW-like anomalies were observed again.

In summary, the SST Hovmoller diagrams show westward propagating anomalies with TIWs characteristics at 23ºW during most of the year, except from February to May when the SST

anomalies showed no propagation and large zonal scales. In the eastern part of the basin, the SST anomalies did not propagate.

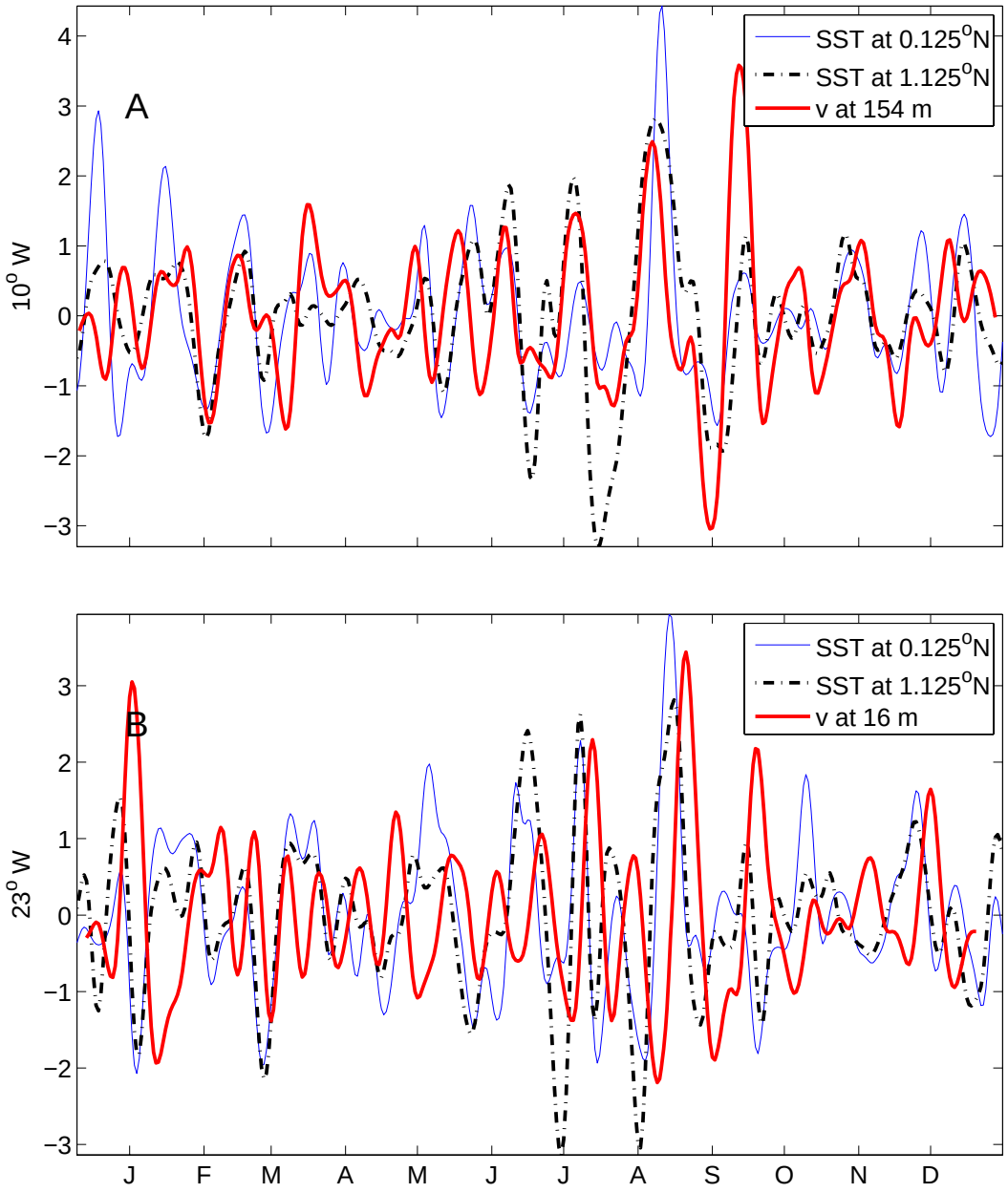

Figure 7: *Panel A:* Normalized and filtered satellite-SST time series from grid points 0.125ºN *(thin line)*, and 1.125N *(dotted lime)* at 10.125ºW, compared to normalized and filtered meridional velocity component data (*thick line*) at 10ºW and 154-m depth. *Panel B*: Same as *panel A*, but for SST time series at 23.125ºW and meridional velocity component at 23ºW and 16-m depth.

The spatial structures of the SST anomalies detected in the Hovmoller diagrams are shown in the 12 panels of figure 6. Panel I illustrates the TIW-like features that occur at the end of December 2001 and beginning of January 2002. During that period, a train of at least three alternate-sign SST anomalies centered at about 1ºN and presenting zonal scales comparable to those of TIWs was observed. The panels II and III (corresponding to February 25 and May 16, 2002) show an example of the non-propagating large scale features detected in Fig. 5.The transition from basin scale anomalies to TIWs is illustrated by the panels IV and V: on May 28, two opposite-sign anomalies were situated at the equator and by June 5, the SST anomalies from the northern hemisphere began to show smaller zonal scales. The SST snapshot of June 15 (panel VI) shows well developed TIWs. West of 10ºW, the SST anomalies exhibit zonal wavelengths of approximately 1,100 km and an antisymmetric phase structure about the equator, both characteristic of TIWs (e.g., Weisberg and Weingartner, 1988; Chelton et al., 2000). The TIW-SST signal was strongest by June 23 (panel VII). East of 10ºW, however, the temperature anomalies are very different, presenting similar periodicities but at larger zonal scales than the SST anomalies west of 10ºW (panels VI, VII and VIII). Around July 17 (panel IX), the antisymmetric structure about the equator of the TIWs became disorganized: in the southern SST anomalies, at about 4ºS, there was a partition of the zonal scale leading to a new zonal scale of roughly 500 km (panels IX and X). In the northern hemisphere, the SST anomalies are no longer round-shaped**,** as it is the case on the July 27 snapshot (panel X). By the end of August (panel XI), the TIW season, as represented in the SST snapshots, was over. Later, in October and November 2002, SST anomalies with the characteristics of TIW were however again observed around 18ºW (panel XII).

The variability in the satellite SST series at 10ºW and 23ºW (Fig. 7) does show similarities to that of the meridional velocity data fluctuations. This is especially true for TIW events at 23ºW (Fig. 7b). At 23ºW, there is a time-lag between the SST and the meridional velocity records at 16 m depth, with the SST leading by 5–10 days, depending on the particular TIW event (Fig. 7b). There is however no phase lag between the SST and the meridional velocity at 120 m (not illustrated). This is not surprising considering that the phase propagation of the meridional velocity component is upward with the TIW- signal in the meridional velocity component at 120 m depth happening to be in phase with the TIW-SST signal. Similarly, at 10ºW, there is also no time-lag between SST-TIWs events and the 154 m depth velocity time series (Fig.7a).

2.4. Discussion and Conclusions

In the near-surface velocity data set at 10ºW and 23ºW, signals at subseasonal time-scales are less conspicuous in the zonal component than in the meridional component. There is, however, one exception at 23ºW: fluctuations with periodicities of 5–7 days which showed a near-surface temperature signature as well. The relation between temperature and zonal velocity component cannot be surmised to the zonal displacements since zonal temperature gradients are unlikely to be important on a 7-day time scale. Since the largest amplitudes in temperature (2.5ºC) are seen at the thermocline depth (~60 m), it is most likely that these near-surface temperature fluctuations are linked to vertical water movements. The temperature fluctuations in the 5- to 10-day range are especially interesting since they mostly occur during June and July simultaneously with the seasonal upwelling and therefore could contribute to the heat exchange at the base of the mixed layer.

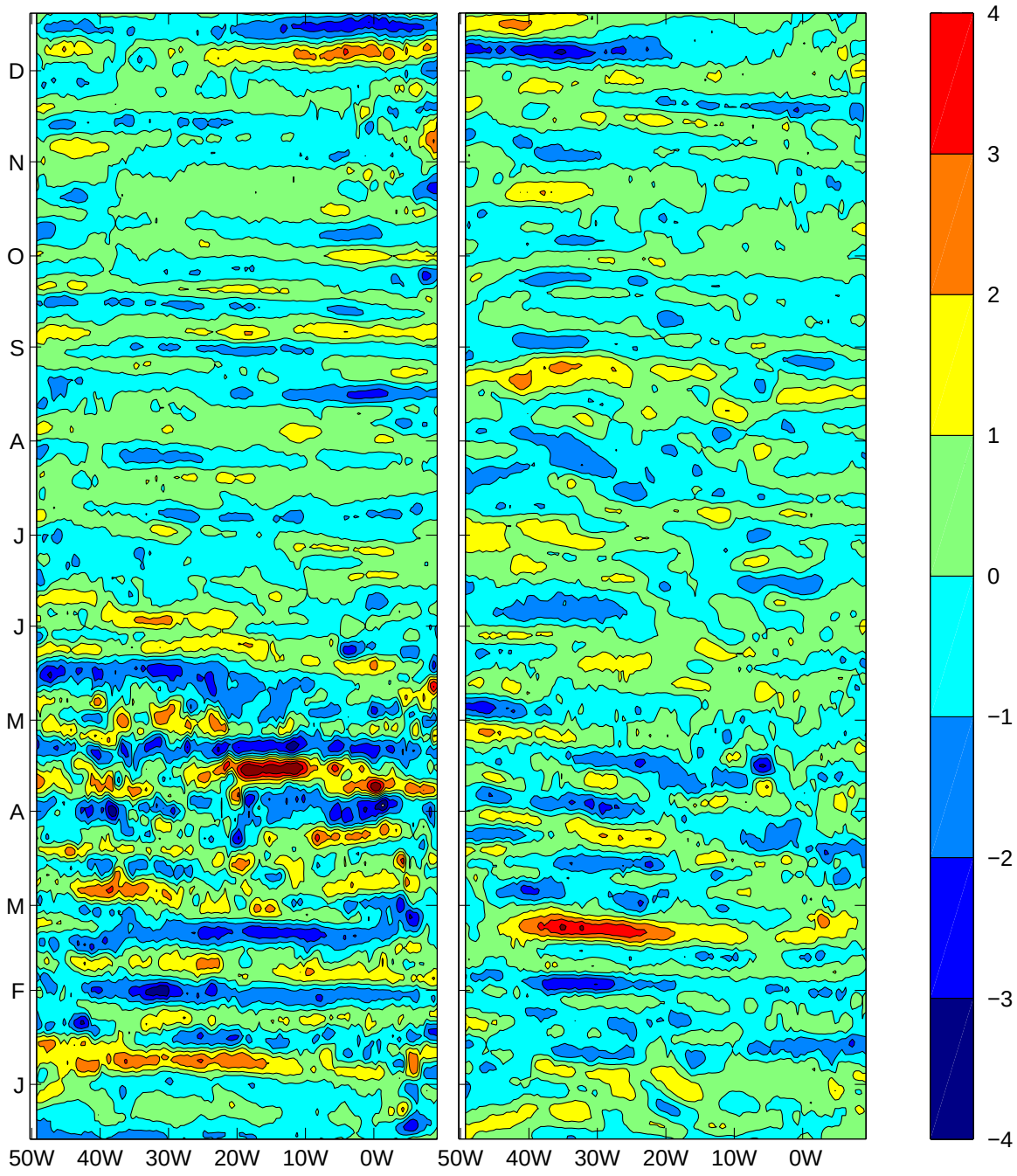

Figure 8: Hovmoller diagrams of zonal (left) and meridional (right) wind velocity components at latitudes 0.25º N. The wind velocity data has been band pass filter to retain variability in the 5 to 38 day band. The velocity scale is in m/s and the months on the y-axis are set in the first day of each month.

An important part of the variability observed at both locations in the near-surface meridional velocity component is due to oscillations with an approximately 14-day periodicity (Fig. 4). These 14-day-period oscillations are present exclusively in the meridional component, show a clear upward phase propagation and downward energy radiation, reminiscent of a first mode mixed Rossby–gravity wave of similar characteristics to what was observed in the western Pacific Ocean by Zhu et al. (1998). In Zhu et al. (1998), the wave resulted from a northerly wind burst crossing the equator. Examination of QuikSCAT surface wind velocity data for the year 2002 in the Atlantic shows great activity at intraseasonal time scales in both horizontal velocity components at large zonal scales (Fig. 8). When comparing the QuikSCAT wind velocity data to the current velocity data, however, we could not find a perfect correspondence for all individual events with either wind velocity component. When there is no correspondence, this does not mean that the 14-day period oscillation in the meridional velocity is not due to wind fluctuations: it could indeed be set in motion by the wind initially and then persists as a free wave by its inherent dynamics. The SST data between February and May 2002 showed non-propagating large scale anomalies and, even though these anomalies occurred simultaneously with the 14-day period oscillation in the meridional velocity component, they could not be directly related to the first baroclinic mode mixed Rossby-gravity wave observed in the velocity measurements. This is because i) the SST time series has larger periods than the meridional current-velocity time series and ii) the SST signature of a mixed Rossby gravity wave should show an antisymmetric temperature structure about the equator and the SST anomalies of boreal spring 2002 have a symmetric structure about the equator.

TIWs can easily be detected in SST snapshots by their equatorially antisymmetric phase structure and by their zonal scale of ~1100 km (e.g., Chelton et al., 2000). This situation is

observed three times in the year, one at the beginning of 2002, one in summer 2002, and another one in fall 2002. The formation of TIWs depends on the intensification of zonal equatorial currents (e.g., Kessler 2004) and, since there is a second intensification of the winds and currents in the Atlantic during the November-December period (e.g., Provost et al., 2004; Okumura and Xie, 2006), it was not surprising to observe TIW-like events during November 2002. The TIW events in early January, however, can only be explained in terms of interannual variability. Indeed, an analysis of interannual variability in the equatorial Atlantic by Provost et al. (2006) showed that the winter 2001-2002 had the coldest SSTs, the strongest westward winds, and the steepest zonal slope anomaly, when compared with other winters from 1993 to 2003. These anomalous conditions could have also led to anomalously stronger equatorial currents which in turn could have favored the generation of TIWs in winter 2001-2002. Overall, variability in both the SST and the meridional velocity component was dominated by TIWs-like events throughout most of the year, except from February to mid May. During the latter, the agreement between the zonal scales of the SST and wind velocity anomalies as well as between the 14-day period in wind and current meridional velocity suggests that the variability was wind forced.

The antisymmetric phase structure of the TIW events during the summer of 2002 was only observed from early June to mid-July. Afterward, the anomalies north of the equator became disorganized and the anomalies to the south reduced their zonal scale by half and disappeared soon after. These changes are accompanied by a reduction of the phase velocity of SST anomalies at the equator (see Hovmoller diagrams on Fig. 6). Despite the fact that the SST anomalies no longer had the antisymmetric shape of TIWs, the SST time-series and the meridional velocity component at 23ºW went on showing perturbations with the same periodicity, therefore implying that the TIWs had not died off. Indeed, SST signatures of TIWs

in the Pacific Ocean have been shown to persist after the velocity perturbations have died off with the propagation of the anomalies resulting from advection by the background flow (Contreras, 2002). Also in the Pacific Ocean, there is an apparent difference in the periodicity of TIWs, depending on the quantity under consideration: SST, altimetric sea surface height, or current velocity (Kessler, 2004). This is not the case in the Atlantic; time-series of SST at 10ºW and 23ºW have oscillations induced by TIWs with the same periodicity as the TIW- induced signatures in the near-surface velocity records (Fig. 7). This fact made the comparison between the velocity and SST data sets straightforward. Lyman et al. (2006) found that the differences in the periodicity of TIWs in the Pacific detected on off-equatorial temperature records and on meridional velocities at the equator, were the result of two types of TIWs coexisting at the same time with distinct periods, dynamical structures, and latitudinal extent. During the deformation of TIWs in mid July, the reduction of the phase velocity of the SST-anomalies at the equator suggests the development of a different TIW. However, there is no change in the period.

Finally, another intriguing set of SST anomalies were the ones found east of 10ºW in the Gulf of Guinea. Although they presented the same periodicities as in the west, their temperature structure had different characteristics: the zonal scale was larger than that of TIWs observed in the west and they did not propagate (Fig. 5 and 6). Whether all these different SST-TIW anomalies expressions share the same dynamics or not, whether they are all part of a single instability process or of different types and/or regions of TIW generation, are questions that remain to be explored.